AMERICAN SOCIETY FOR MICROBIOLOGY | Antimicrobial Agents and Chemotherapy®

CLINICAL THERAPEUTICS

Population Pharmacokinetic Modeling and Probability of Target Attainment of Ceftaroline in Brain and Soft Tissues

Victória Etges Helfer,[a] Alexandre Prehn Zavascki,[b,c] Markus Zeitlinger,[d] Bibiana Verlindo de Araújo,[a] Teresa Dalla Costa[a]

[a]Pharmaceutical Sciences Graduate Program, Federal University of Rio Grande do Sul, Porto Alegre, Brazil
[b]Infectious Diseases Service, Hospital de Clínicas de Porto Alegre, Porto Alegre, Brazil
[c]Department of Internal Medicine, Universidade Federal do Rio Grande do Sul, Porto Alegre, Brazil
[d]Department of Clinical Pharmacology, Medical University of Vienna, Vienna, Austria

ABSTRACT Ceftaroline, approved to treat skin infections and pneumonia due to methicillin-resistant *Staphylococcus aureus* (MRSA), has been considered for the treatment of central nervous system (CNS) infections. A population pharmacokinetic (popPK) model was developed to describe ceftaroline soft tissue and cerebrospinal fluid (CSF) distributions and investigate the probability of target attainment (PTA) of the percentage of the dosing interval that the unbound drug concentration exceeded the MIC (%$fT_{>MIC}$) to treat MRSA infections. Healthy subjects' plasma and microdialysate concentrations from muscle and subcutaneous tissue following 600 mg every 12 h (q12h) and q8h and neurosurgical patients' plasma and CSF concentrations following single 600-mg dosing were used. Plasma concentrations were described by a two-compartment model, and tissue concentrations were incorporated as three independent compartments linked to the central compartment by bidirectional transport (clearance in [CL_{in}] and CL_{out}). Apparent volumes were fixed to physiological interstitial values. Healthy status and body weight were identified as covariates for the volume of the central compartment, and creatinine clearance was identified for clearance. The CSF glucose concentration (GLUC) was inversely correlated with $CL_{in,CSF}$. Simulations showed a PTA of >90% in plasma and soft tissues for both regimens assuming an MIC of 1 mg/L and a %$fT_{>MIC}$ of 28.8%. Using the same target, patients with inflamed meninges (0.5 < GLUC ≤ 2 mmol/L) would reach PTAs of 99.8% and 97.2% for 600 mg q8h and q12h, respectively. For brain infection with mild inflammation (2 < GLUC ≤ 3.5 mmol/L), the PTAs would be reduced to 34.3% and 9.1%, respectively. Ceftaroline's penetration enhanced by meningeal inflammation suggests that the drug could be a candidate to treat MRSA CNS infections.

KEYWORDS MRSA infection, PTA, brain penetration, ceftaroline, peripheral tissue penetration, popPK model

Ceftaroline, the active metabolite of the prodrug ceftaroline fosamil, is a cephalosporin approved for the treatment of complicated skin and soft tissue infections (cSSTIs) and community-acquired pneumonia (1). In contrast to the majority of cephalosporins, ceftaroline presents activity against multiresistant Gram-positive microorganisms, including methicillin-resistant *Staphylococcus aureus* (MRSA) (2). Due to the increased prevalence of infections caused by MRSA and owing to the risks and toxicity of most of the antimicrobial options available, ceftaroline has been considered for the treatment of nonapproved conditions such as meningitis (3–5). *S. aureus* meningitis accounts for 4.9 to 6.4% of total cases and presents a high mortality rate depending on the infection source (hematogenous source, 43 to 50%; postsurgically, 14 to 25%) (6).

There are few reported cases of the clinical success of central nervous system (CNS) infections treated with ceftaroline (4, 7, 8). Recent reports of neurosurgical patients

Address correspondence to Teresa Dalla Costa, dalla.costa@ufrgs.br.

The authors declare a conflict of interest. This work was partially financed by a grant from Pfizer (2018 Anti-Infectives ASPIRE, # WI242215). A.P.Z., B.V.d.A., and T.D.C. have received research grants from Pfizer.

[This article was published on 25 August 2022 with errors in the affiliation line. The affiliation line was corrected in the current version, posted on 1 September 2022.]

Received 26 May 2022
Returned for modification 8 July 2022
Accepted 2 August 2022
Published 25 August 2022

TABLE 1 Summary of the demographic and clinical characteristics of the subjects included in popPK modeling[a]

Parameter	Value for group	
	Healthy volunteers[d]	Neurosurgical patients[b]
No. of male/no. of female subjects	12/0	5/4
Median age (yrs) (SD)	27.5 (8.2)	71 (15.6)
Median wt (kg) (SD)	74.5 (12.1)	79 (17.2)
Median creatinine clearance[c] (mL/min) (SD)	145 (22.2)	108 (41.4)
Median CSF glucose concn (mmol/L) (SD)	NA	3.9 (0.9)
Median CL_{EVD} (mL/h) (SD)	NA	5.42 (3.1)

[a]CSF, cerebrospinal fluid; CL_{EVD}, flow rate of the external ventricular drain; NA, not applicable.
[b]Data from Chauzy et al. (9).
[c]Calculated by the Cockcroft-Gault equation.
[d]Data from Matzneller et al. (10).

who had an external ventricular drain (EVD) that allowed sampling indicated that the drug shows low penetration in the cerebrospinal fluid (CSF) (9). However, no data are available concerning the evaluation of pharmacokinetic-pharmacodynamic (PK/PD) target attainment of this drug in CNS infections.

Similarly, limited data are available regarding the ceftaroline peripheral tissue distribution (10, 11). Although many studies have demonstrated the effectiveness of this drug for the treatment of cSSTIs, all were conducted using plasma concentrations as a surrogate for biophase concentrations (12, 13). One study has shown low unbound concentrations of ceftaroline in the extracellular fluid of muscle and subcutaneous tissues, determined by microdialysis, in comparison to plasma levels, indicating that free plasma concentrations may overestimate pharmacologically active concentrations at the infection site (10).

The development of a population pharmacokinetic (popPK) model combined with Monte Carlo simulations could be a powerful tool to determine the optimal dosage regimen to maximize the likelihood of reaching the necessary exposure to treat infections (14). This is especially useful in studies with a limited number of patients, commonly associated with CNS infections, where the model can be used to make predictions of untested scenarios (15).

Intending to evaluate the adequacy of ceftaroline for the treatment of CNS and soft tissue infections, here, we describe the development of a popPK model built using free peripheral concentrations collected by microdialysis in muscle and subcutaneous tissue, previously reported by Matzneller and colleagues (10), along with CSF free concentrations obtained from neurosurgical patients, previously reported by Chauzy and colleagues (9).

RESULTS

Patients and data. The demographics and clinical characteristics of the 12 volunteers and 9 neurosurgical patients are summarized in Table 1. The overall median age was 35 years, with most older subjects belonging to the neurosurgical group. Women were included only in the patient group, which presented a broader range of creatinine clearance (CL_{cr}) values. The overall median CL_{cr} was 125.7 mL/min.

Pharmacokinetic analysis. Totals of 323 plasma concentrations (274 from healthy volunteers and 49 from neurosurgical patients); 289 and 281 microdialysate concentrations in muscle and subcutaneous tissues, respectively; and 54 CSF concentrations were included in the population analysis. Plasma concentrations were best described by a two-compartment model parameterized in terms of clearance (CL), the central volume of distribution (V_1), the peripheral volume of distribution (V_2), and intercompartmental clearance (Q). Tissue concentrations were incorporated into the model as individual compartments, with volumes fixed as interstitial physiological values (16, 17). These compartments were linked to the central compartment with bidirectional transport, parameterized as intercompartmental clearance in and out (Q_{in} and Q_{out}, respectively) (Fig. 1). Interindividual variability (IIV) was described by an exponential model and was then estimated for V_1, CL,

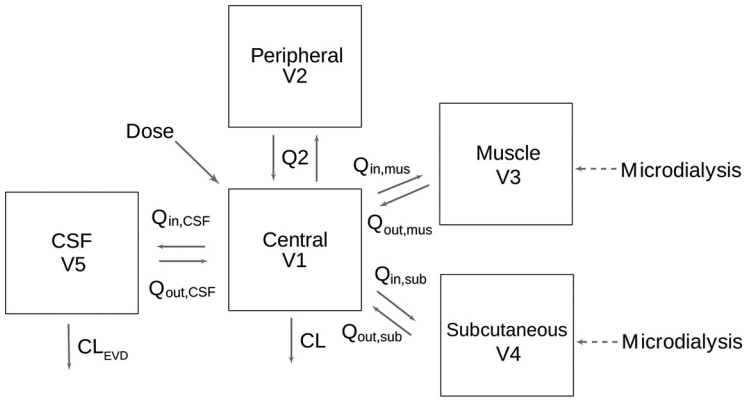

FIG 1 Ceftaroline structural popPK model. V1, volume of the central compartment; V2, peripheral volume of distribution; V3, volume of the muscle tissue compartment; V4, volume of the subcutaneous tissue compartment; CL, clearance from the central compartment; CL_{EVD}, elimination of ceftaroline from the CSF via an external ventricular drain; Q2, intercompartmental clearance between the central and peripheral compartments; Q_{in}, intercompartmental clearance into the tissue; Q_{out}, intercompartmental clearance out of the tissue.

$Q_{in,muscle}$, $Q_{in,subcutaneous}$, and both $Q_{in,CSF}$ and $Q_{out,CSF}$, where the latter two shared the same IIV. An additive-error model for each plasma, muscle, subcutaneous tissue, and CSF concentration was sufficient to describe the residual unexplained variability. The loss of CSF by an EVD was considered by including it as a fixed value of its actual rate for each patient (CL_{EVD}) (9).

Concerning the covariate analysis, the inclusion of CL_{cr} on CL leads to a significant decrease in the objective function value (OFV) (ΔOFV, 14.50) and explains the variability on this parameter by reducing it from 23.7% to 17.5%. Patient status and weight were related to a decrease in the IIV from 29.7% to 16.4% (ΔOFV, 13.23 and 11.51, respectively). The inclusion of the glucose concentration (GLUC) in $Q_{in,CSF}$ leads to a reduction of the IIV from 100% to 58.1% (ΔOFV, 26.165).

The final model parameters including the covariates were expressed as follows:

$$\mathrm{CL(L/h)} = 12.8 \times e^{0.00495 \times (\mathrm{CL_{cr}} - 125.7)}$$

$$V_1\,(\mathrm{L}) = 18 \times (1 + 0.482 \times \text{healthy status}) \times e^{0.0119 \times (\text{weight} - 76.5)}$$

$$Q_{\mathrm{in,CSF}}(\mathrm{L/h}) = 0.00142 \times e^{-0.737 \times (\mathrm{GLUC} - 3.9)}$$

The inverse correlation found between $Q_{in,CSF}$ and GLUC can be observed in Fig. 2, which includes data from the observed neurosurgical patients and 1,000 simulated individuals assuming a random distribution of GLUC of between 3.5 and 6.5 mmol/L.

The parameters for the final popPK model are shown in Table 2, together with uncertainties and distributions describing the IIV in model parameters. Model parameters were estimated with good precision, and diagnostic plots showed a good agreement between the observed and predicted data (Fig. 3 and 4). The prediction-corrected visual predictive check (pcVPC) indicated adequate goodness of fit and good predictive performance of the final popPK model for all tissues investigated (Fig. 5).

Simulations. The PTA-versus-MIC profiles corresponding to Monte Carlo simulations of the groups with normal renal function and different stages of meningeal inflammation for the two different dosing regimens for a PD target of a percentage of the dosing interval that the unbound drug concentration exceeded the MIC (%$fT_{>MIC}$) of 34.7% are represented in Fig. 6. Simulations for the other groups and targets of %$fT_{>MIC}$ of 26.8% and 30.7% are illustrated in Fig. S1 to S11 in the supplemental material.

Based on the free plasma concentrations, the percentages of simulated patients achieving the ceftaroline target PK/PD index were above 90% for a 2-mg/L MIC across

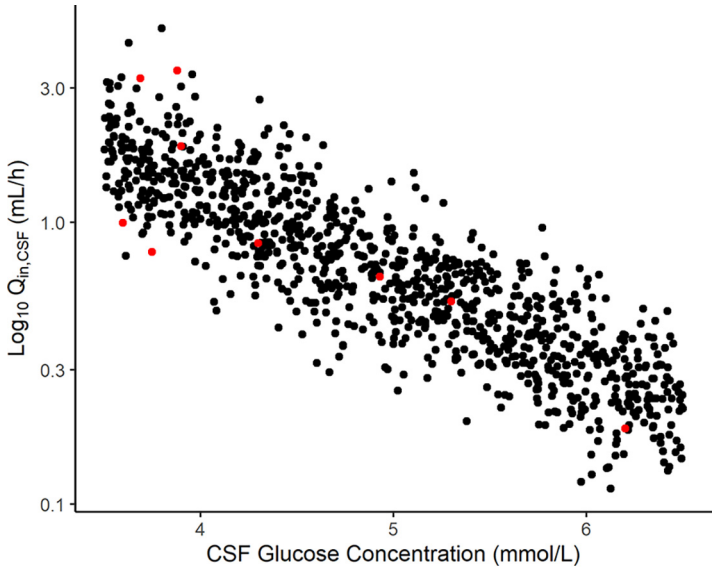

FIG 2 Correlation between intercompartmental clearance into the CSF (Q_{in}) and the CSF glucose concentration. Red circles represent the observed data, and black circles represent the simulated patients.

all groups and dosing regimens evaluated. On the other hand, based on free ceftaroline muscle and subcutaneous tissue concentrations, the desired target of a ≥90% PTA for an MIC of 2 mg/L was reached across all tested groups only when using 600 mg through a 2-h intravenous (i.v.) infusion three times a day. When the same amount of the drug was administered as a 1-h i.v. infusion twice a day, the percentage of simulated patients with normal renal function achieving $\%fT_{>MIC}$ targets of 28.8%, 30.7%, and 34.7% were 95.3%, 81.8%, and 52.0% for muscle and 98.7%, 93.1%, and 73.0% for

TABLE 2 Parameter estimates of the final ceftaroline population pharmacokinetic model[a]

Parameter	Estimated value (% RSE)	Bootstrap mean estimated value (95% CI)[b]	% CV for IIV (% RSE)	Bootstrap mean % CV (95% CI)[a]
CL (L/h)	12.8 (4.3)	12.75 (11.73 to 13.86)	18.4 (16.4)	17.5 (12.3 to 22.0)
V_1 (L)	18.0 (5.9)	17.97 (15.83 to 20.03)	16.3 (26.2)	14.8 (7.3 to 20.4)
Q_2 (L/h)	4.57 (5.5)	4.47 (3.31 to 6.67)		
V_2 (L)	8.11 (11.3)	7.93 (5.69 to 9.72)		
$Q_{in,muscle}$ (L/h)	5.96 (13.2)	5.99 (4.63 to 7.77)	30 (22)	28.9 (15.6 to 40.6)
$Q_{out,muscle}$ (L/h)	11.4 (9.1)	11.35 (9.32 to 13.96)		
V_{muscle} (L)	3.91 fix	3.91 (3.91 to 3.91)		
$Q_{in,subcutaneous}$ (L/h)	3.3 (13.5)	3.34 (2.41 to 4.58)	33.3 (21.6)	31.7 (18.5 to 39.9)
$Q_{out,subcutaneous}$ (L/h)	5.69 (8.7)	5.71 (4.38 to 7.32)		
$V_{subcutaneous}$ (L)	2.29 fix	2.29 (2.29 to 2.29)		
$Q_{in,CSF}$ (mL/h)	1.42 (23.3)	1.48 (0.90 to 2.39)	57.6 (30.6)	59.1 (20.6 to 95.9)
$Q_{out,CSF}$ (mL/h)	16.3 (22.2)	16.39 (9.42 to 24.60)	57.6 (30.6)	59.1 (20.6 to 95.9)
V_{CSF} (L)	0.15 fix	0.15 (0.15 to 0.15)		
$\theta_{healthy\ status}$	0.481 (30.1)	0.529 (0.117 to 0.978)		
θ_{wt}	0.012 (28.3)	0.0123 (0.0045 to 0.0195)		
θ_{CrCL}	0.00495 (26.1)	0.00511 (0.0031 to 0.0080)		
$\theta_{glucose}$	−0.737 (15.7)	−0.803 (−1.61 to −0.413)		
Plasma additive error (mg/L)	0.155 (4.4)	0.151 (0.123 to 0.176)		
Muscle additive error (mg/L)	0.318 (4.3)	0.315 (0.270 to 0.360)		
Subcutaneous tissue additive error (mg/L)	0.324 (4.4)	0.322 (0.283 to 0.364)		
CSF additive error (mg/L)	0.518 (10.7)	0.486 (0.266 to 0.754)		

[a]CL, clearance; V_1, central volume of distribution; Q_2, intercompartmental clearance from the central compartment to the peripheral compartment; V_2, peripheral volume of distribution; Q_{in}, intercompartmental clearance from the central compartment to the indicated tissue; Q_{out}, intercompartmental clearance from the indicated tissue compartment to the central compartment; fix, fixed value; RSE, relative standard error; CV, coefficient of variation; CI, confidence interval; theta symbol, estimated theta for the covariate; CrCL, creatinine clearance; wt, weight.

[b]Bootstrap analysis was performed with 1,000 data sets, with 940 successful runs.

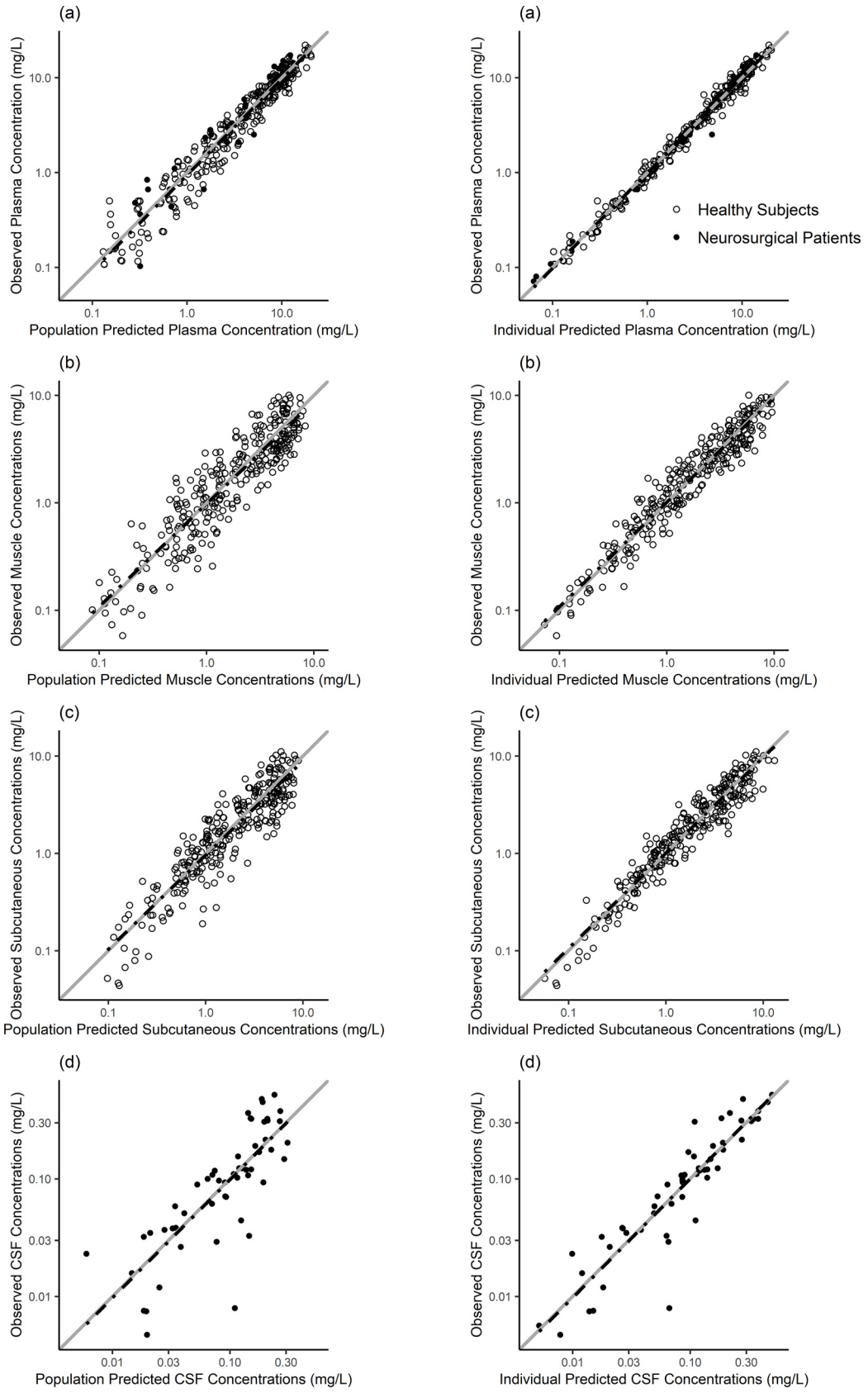

FIG 3 Observed versus population-predicted (left) and individual-predicted (right) ceftaroline concentrations in plasma (a), muscle (b), subcutaneous tissue (c), and CSF (d). The solid gray lines represent the line of identity ($x = y$), and the dashed black lines represent the linear regression line of fit.

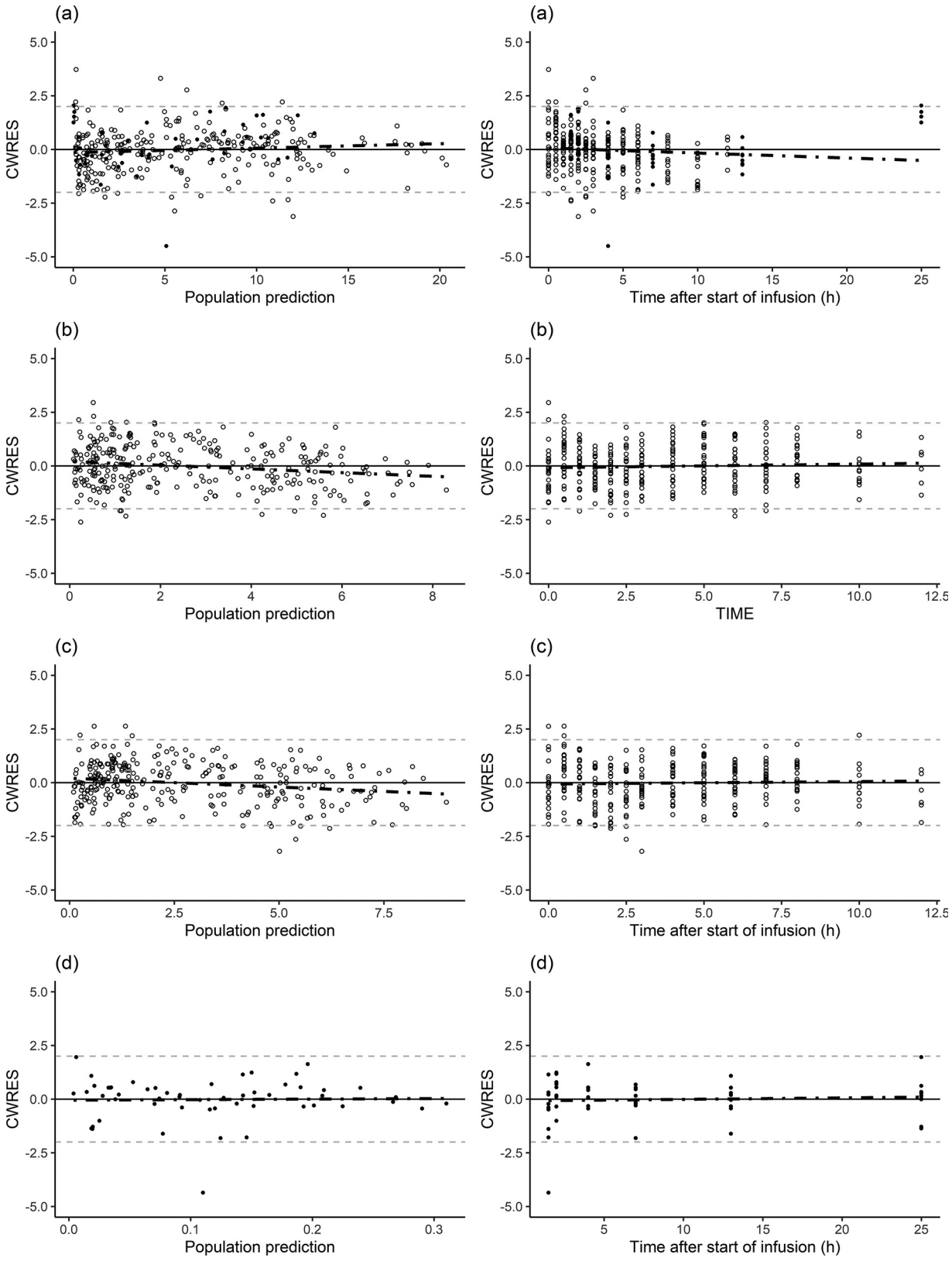

FIG 4 Conditional weighted residual error (CWRES) versus population-predicted ceftaroline concentrations (left) and versus time after the last dose (right) for plasma (a), muscle (b), subcutaneous tissue (c), and CSF (d). Individual data points are indicated by filled circles (neurosurgical patients) or open circles (healthy subjects). The dashed black lines represent a smooth line, and the horizontal solid gray lines are the zero line.

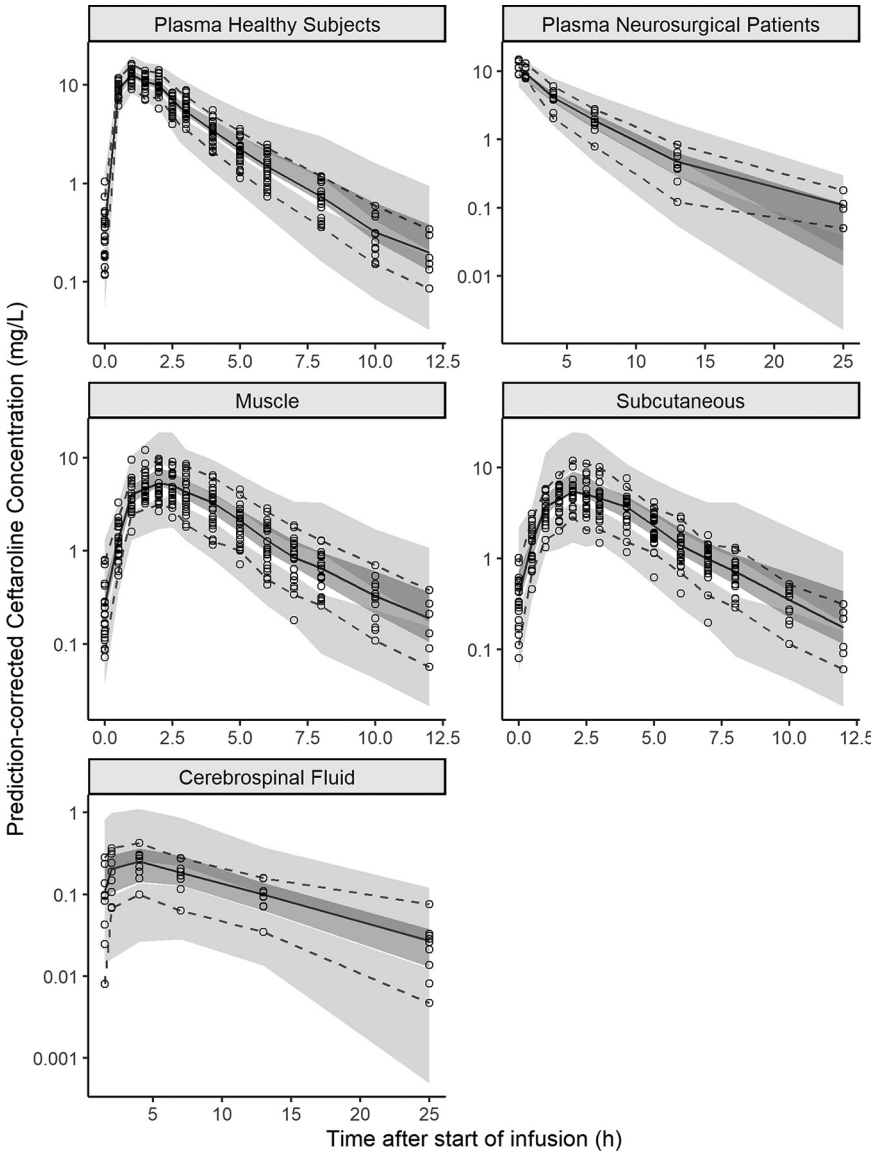

FIG 5 Prediction-corrected visual predictive check (pcVPC) for ceftaroline in plasma of healthy subjects (top left), plasma of neurosurgical patients (top right), muscle tissue (middle left), subcutaneous tissue (middle right), and cerebrospinal fluid (bottom) based on 1,000 simulated data sets. Circles represent the observed data. The shaded areas are the 95% confidence intervals for the 2.5th (light gray), 50th (dark gray), and 97.5th (light gray) percentile prediction intervals based on the simulated data. The solid black lines represent the median observed concentration, and the dashed black lines represent the observed 2.5th and 97.5th percentiles.

subcutaneous tissue, respectively. For the group with impaired renal function receiving 400 mg twice a day, the percentage of simulated patients achieving %$fT_{>MIC}$ targets of 28.8%, 30.7%, and 34.7% were 98.4%, 89.2%, and 57.5% for muscle and 99.5%, 97.4%, and 85.3% for subcutaneous tissue, respectively.

Considering ceftaroline CSF concentrations for the treatment of CNS infections, the probabilities of target attainment are lower for the no-inflammation state in the meninges than for the inflamed state. Simulated patients with an absence of inflamed meninges reached concentrations that may not be appropriate to treat CNS infections independently of the renal function status and dosing regimen evaluated. However, when considering the inflamed state of the meninges, for an MIC of 1 mg/L and a dosing interval of 12 h, the percentages of simulated patients with normal renal function achieving %$fT_{>MIC}$ targets of 28.8%, 30.7%, and 34.7% were 97.2%, 96.9%, and 96.3%,

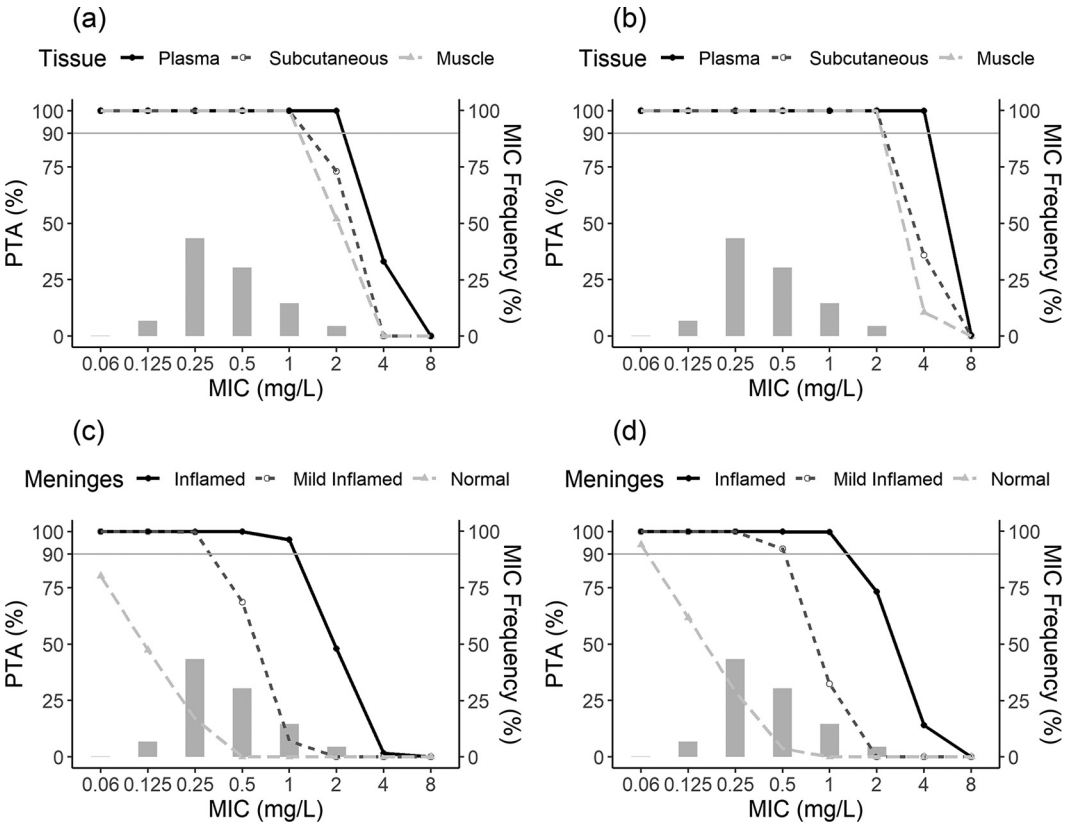

FIG 6 Probability of target attainment (PTA) for 1,000 simulated patients with normal renal function achieving a $\%fT_{>MIC}$ target of 34.7% for MRSA by MIC following the administration of ceftaroline fosamil at 600 mg q12h as a 1-h i.v. infusion (a and c) or 600 mg q8h as a 2-h i.v. infusion (b and d), overlaid with the ceftaroline MIC distribution for MRSA from EUCAST (light gray bars). The top panels are representative of unbound plasma (solid black lines with closed circles), muscle (dashed light gray lines with triangles), and subcutaneous tissue (dashed gray lines with open circles). The bottom panels are representative of cerebrospinal fluid depending on the meningeal status: inflamed (solid black lines with closed circles), mildly inflamed (dashed gray lines with open circles), and normal (dashed light gray lines with triangles).

respectively, whereas for the dosage regimen with a shorter interdose interval, the achieved PTA was 99.8% for all three targets.

DISCUSSION

Based on data from previously published studies with healthy volunteers and neurosurgical patients, it was found that the patient status can influence the plasma disposition of the drug as a result of an increased volume of distribution in the patient population. It was shown that ceftaroline reaches sufficient free concentrations in soft tissues for the treatment of MRSA-related infections. Additionally, our results showed that the penetration of ceftaroline into the CSF may depend on the degree of meningeal inflammation, where patients with inflamed meninges present better penetration, leading to higher probabilities of reaching the PD target for MRSA infections.

A two-compartment model was found to adequately describe plasma ceftaroline concentrations, in agreement with other models reported in the literature (11, 18, 19). Also, similar to those models, the covariate analysis showed that clearance was directly correlated with creatinine clearance, which can be explained by the renal elimination pathway of this antimicrobial (20). Additionally, weight was identified as an important covariate for the central volume of distribution, where heavier patients would present an increased volume of distribution. Furthermore, neurosurgical patients showed a higher volume of distribution (26.7 L) than healthy subjects (18 L). This phenomenon has been described in previous models for ceftaroline (18) and is in agreement with

the literature as cephalosporins and β-lactams usually present a higher volume of distribution in patients than in healthy subjects (21, 22).

The time to the maximum free concentration of the drug (T_{max}) in tissues occurred after the one observed in plasma. This pattern of delayed distribution to the tissues was modeled with bidirectional transport parameterized with clearance in (CL_{in}) and CL_{out}, assuming one additional compartment for each observed tissue. Due to the nature of the microdialysis data, which leads to richer information on drug tissue concentrations, and due to the small number of CSF samples, the volumes of tissue compartments were fixed to the interstitial physiological values (16, 17), aiming to stabilize the model predictions. This strategy has previously been used in analyses of tissue concentrations, such as lung and central nervous system concentrations (23–26).

The model-estimated ratios of ceftaroline penetration into the muscle and subcutaneous tissues were 0.52 and 0.58, respectively. Although the drug exposures were similar between these two tissues, they showed important differences in the PTA analysis (Fig. 6). For instance, following ceftaroline fosamil as a 1-h i.v. infusion of 600 mg twice daily, the target of 30.7% for the 2-mg/L MIC was reached in the subcutaneous tissue (93.1%) but not the muscle (81.8%). This highlights the importance of characterizing the disposition of drugs at different sites of infection once different exposures lead to different outcomes.

The observed CSF penetration ratio of about 9%, as expected, was lower than the penetration ratios observed in peripheral tissues. Despite this low penetration, an important inverse correlation was found between glucose CSF concentrations and intercompartmental clearance to the CSF ($Q_{in,CSF}$), as previously reported (9) (Fig. 2). The higher the glucose levels in CSF, the lower the penetration of ceftaroline into the CNS. Since hypoglycorrhachia (glucose level of $<$40 mg/dL or 2.22 mmol/L) (27) is commonly associated with infections such as meningitis, this clinical parameter was further explored under circumstances not observed in the patients used to build the model, who showed CSF glucose concentrations no lower than 3.6 mmol/L. Assuming a uniform distribution, three stages of CSF glucose concentrations were simulated. The group with an absence of inflammation (mean glucose levels of 5 mmol/L) would present a median ceftaroline penetration in the CSF of 4%. The group with mildly inflamed meninges (mean glucose levels of 2.8 mmol/L) would present a median penetration of about 19%, while in the group with inflamed meninges (mean glucose levels of 1.2 mmol/L), ceftaroline penetration would be higher, with a median of approximately 62%. These different degrees of CSF exposure resulted in quite pronounced differences in the PTAs among the three stages of inflammation. For an MIC of 1 mg/L and a % $fT_{>MIC}$ target of 34.7%, the percentages of simulated patients with normal renal function and inflamed meninges who would attain the PK/PD target were 99.8% and 96.3% for three-times-daily and twice-daily doses, respectively. The reached percentages for simulated patients with mildly inflamed meninges were 32.3% and 7.2% for three-times-daily and twice-daily doses, respectively, while none of the simulated patients with noninflamed meninges reached the target for both dosing regimens. Patients with mild renal impairment and inflamed meninges receiving the three-times-daily dosage regimens reached better results, with 89.8% of the simulated patients reaching the %$fT_{>MIC}$ target of 34.7% at a higher MIC of 2 mg/L. The same pattern was observed in the simulated patients with impaired renal function, where at an MIC of 2 mg/L, the PTA was 95.5%. However, when adjusting for the recommended dose of 400 mg, the PTAs were similar to those encountered in simulated patients with normal renal function (see Fig. S1 to S11 in the supplemental material).

This pattern of poor CNS penetration into intact meninges and increased penetration into inflamed meninges has been reported previously for other antimicrobials (28, 29). Vancomycin, the antimicrobial recommended by the Infectious Diseases Society of America for the treatment of MRSA meningitis, is one of them (23, 30, 31). One study conducted with adult patients presenting CSF characteristics that strongly suggested a diagnosis of bacterial meningitis, accompanied by a very low glucose concentration

(mean value of <0.5 mmol/L), showed good CSF penetration of vancomycin (approximately 30%) (32). Similar results were reported in another study with patients with postneurosurgical meningitis that compared intermittent and continuous infusion regimens (CSF/serum ratios of 24.84% and 27.39%, respectively) (33). In cases of noninflamed meninges, such as ventriculitis, the reported vancomycin penetration is much lower (23, 31). Blassmann and collaborators (31) reported a CSF/serum ratio of 3% in patients with an EVD implanted who had proven or suspected EVD-associated ventriculitis and were receiving vancomycin as a prolonged infusion over 4 h.

Due to concerns about vancomycin nephrotoxicity, ceftaroline has been used off-label to treat patients with different CNS infections. Some case reports confirm the success of ceftaroline in the treatment of CNS infections foreseen in the present study. Cies and colleagues (7) reported an MRSA ventriculopleural shunt infection successfully treated with ceftaroline. The patient initially received vancomycin and ceftriaxone, with the latter being replaced by ceftaroline on the third day of therapy. The CSF culture was sterilized within 24 h after the addition of ceftaroline. Also, simultaneous serum and CSF concentrations determined at steady state showed a CSF penetration ratio of between 2.4% and 7.6%. Roujansky and collaborators (8) reported a similar case where a patient presented with a ventriculostomy-related infection caused by multidrug-resistant *Staphylococcus epidermidis*. CSF sterilization was reached 6 days after the start of ceftaroline treatment, with a reported CSF penetration ratio of 2.6 to 4.8%. Four cases of bacterial meningitis caused by *Streptococcus pneumoniae* and one caused by methicillin-sensitive *S. aureus* treated with ceftaroline were reported by Sakoulas et al. (4). Clinical success was observed in 4 of the patients, who received treatment with 600 mg three times daily. The only case that required alternative therapy was under a dosing regimen of 600 mg twice daily. These findings are in line with our results since the PTA analysis reported here showed better results with more frequent dosing (three times daily) than with twice-daily doses.

The importance of measuring antimicrobial concentrations at the site of infection has been the topic of discussion in several studies (24, 34, 35). Our results endorse this notion. The PK/PD target of a 2-log kill ($fT_{>MIC}$ of 34.7%) is reached in 100% of the simulated patients with normal renal function and a bacterial MIC of 2 mg/L when free plasma concentrations are used. However, PTAs of 60.1% and 77.7% are observed in muscle and subcutaneous tissues, respectively, for twice-daily dosing since these tissues showed almost half of the exposure observed in plasma (penetration ratios of 0.52 and 0.58, respectively). These findings emphasize that predicting efficacy and guiding dosing regimen selection based solely on free plasma concentrations could lead to treatment failures due to efficacy overestimations (36).

Some limitations of the present study are worth mentioning. The simulations based on the inflamed meningeal state should be interpreted carefully because they were based on nonobserved scenarios. Despite the awareness of the increased penetration of drugs through the blood-brain barrier in the presence of inflammation, it is not possible to confirm that the concentrations simulated in these scenarios will be achieved in patients. Furthermore, the use of the CSF glucose concentration as a marker for the diagnosis of CNS infections can be inaccurate, as some patients present this parameter within the normal range despite a diagnosis of meningitis (37). Some findings indicate that the CSF/serum glucose ratio appears to be more adequate than the CSF glucose concentration itself for a more accurate diagnosis (37). For that reason, further studies must be carried out to confirm the findings in the present study, probably including patients with meningitis. Besides this, free concentrations in soft tissues were determined by microdialysis in healthy volunteers. Reports in the literature have shown that some antimicrobials present different degrees of tissue penetration in the presence of an active infection (38). Specifically, for cephalosporins, Sauermann and colleagues (39) have shown that the penetration of cefpirome into the subcutaneous tissue of septic patients was lower than that in healthy subjects as determined by microdialysis (39). Pathophysiological changes, both locally and systemically, such as protein binding, pH, blood flow, or fluid distribution, could lead to differences in the penetration of the

antimicrobial at the site of action (35). Finally, the PK/PD targets used for the simulations are based on unbound serum concentrations, and they may assume different values when free tissue concentrations are considered (40). Therefore, it is important to consider this when extrapolating the soft tissue results in an ongoing active-infection situation.

In conclusion, we present the results of a popPK analysis of ceftaroline concentrations in plasma, free muscle, subcutaneous tissues, and CSF. The simulations performed showed sufficient coverage of the approved doses in soft tissues, while the penetration of ceftaroline into the CSF depends on the degree of meningeal inflammation. The results also indicate that 600 mg of ceftaroline three times a day may be considered for further evaluation as a candidate to treat CNS infections.

MATERIALS AND METHODS

Data. The popPK model was developed using data from two clinical studies (9, 10). The study design and methodologies used to quantify ceftaroline concentrations in the collected samples have been extensively described in those publications (9, 10).

The complete data set, including demographics and individual pharmacokinetic profiles, from the study by Matzneller et al. was available (10). Briefly, that study involved 12 healthy male volunteers who were randomly assigned to 2 groups of 6 individuals each. During the study period, the first group received 600 mg ceftaroline fosamil over a 2-h i.v. infusion with a dosing interval of 8 h (total of 4 doses), while the second group received 600 mg ceftaroline fosamil over a 1-h i.v. infusion with a dosing interval of 12 h (total of 3 doses). Rich total plasma and free microdialysis samples from muscle and subcutaneous tissue were collected at predefined time points after the first and last doses for each dosing regimen.

Data from the study by Chauzy et al. were extracted from the published report (9), where the individual pharmacokinetic profiles were presented using WebPlotDigitizer v.4.5 software (41). The study by Chauzy et al. involved nine neurosurgical patients who required the insertion of an EVD, through which CSF samples were collected. Patients received a single 600-mg dose of ceftaroline fosamil over a 1-h i.v. infusion, and samples from total plasma and free CSF were taken at different time points up to 24 h after the end of the infusion.

Pharmacokinetic analysis. Concentration-time data were analyzed using nonlinear mixed-effects modeling in NONMEM v.7.4.3 (Icon Development Solutions, USA) (42) with Pirana v.3.0.0 (Certara USA, Inc., USA) (43) to keep track of run records and results. Perl-speaks-NONMEM (PsN) v.4.9.0 (44) was used for automating and controlling the runs. R v.4.0.4 and the Xpose4 v.4.7.1 package (45) were used to guide further model building through data visualization and graphical analysis. The first-order condition estimation method with interaction and the ADVAN13 subroutine were employed for all model runs. The data were modeled as log transformed, and plasma concentrations were corrected by 20% plasma protein binding (20). The fraction of the prodrug converted to active ceftaroline was assumed to be 100%, and the ceftaroline dose was set to 530 mg to take into consideration the differences in molecular weights between ceftaroline and ceftaroline fosamil (18). Modeling was performed sequentially, with plasma being modeled first, followed by the insertion of the tissues individually. The microdialysis data were described by the integral over each collection interval instead of a midpoint approach (46).

Both one- and two-compartment structural models were explored. Interindividual variability was evaluated using an exponential variability model, and log-transformed additive- and combined-error models were tested for residual unexplained variability. Model selection was based on the objective function value (OFV) as well as visual inspection of the standard goodness-of-fit plots (47, 48).

Once the base structural model had been determined, the contributions of covariates to population parameter variability were assessed by applying a stepwise forward-addition ($P < 0.05$) and backward-elimination ($P < 0.01$) procedure (49). The covariates tested were age, body weight, gender, serum creatinine concentrations, creatinine clearance (CL_{cr}) estimated by the Cockcroft-Gault equation, patient status (healthy subjects versus hospitalized patients), and CSF protein and glucose concentrations. Covariates were implemented in the model using exponential functions centralized by the median observed value.

The final model was internally validated using a prediction-corrected visual predictive check (pcVPC) and a bootstrap resampling analysis, stratified on the concentration measurement site and study group, with 1,000 replicates.

Simulations. The final popPK model was used to conduct Monte Carlo simulations to assess ceftaroline tissue exposures in the patient population following ceftaroline fosamil doses of 600 mg every 12 h (q12h) and 600 mg q8h, with doses adjusted to 400 mg for the moderate renal impairment category. A total of 1,000 patients were simulated in each of the three categories of renal function and meningeal inflammation status. The simulations were performed using Berkeley Madonna software v.10.2.8 (50). Renal function categories were defined as follows: normal renal function ($80 < CL_{cr} \leq 130$ mL/min), mild renal impairment ($50 < CL_{cr} \leq 80$ mL/min), and moderate renal impairment ($30 < CL_{cr} \leq 50$ mL/min) (20). The meningeal inflammation status was based on the glucose CSF concentration, where the categories were as follows: normal ($3.5 < GLUC_{CSF} \leq 6.5$ mmol/L), mildly inflamed ($2 < GLUC_{CSF} \leq 3.5$ mmol/L), and inflamed ($0.5 < GLUC_{CSF} \leq 2$ mmol/L) (27). The simulated weight included only individuals between 45 and 120 kg. For all simulations, the values of the covariates were assumed to follow a uniform distribution within the designated range for each category.

The $\%fT_{>MIC}$ was calculated for the simulated patients in each dosing regimen and group category at MIC values ranging from 0.06 to 8 mg/L. The PTAs were calculated as the percentages of the 1,000

simulated patients who met the MRSA PK/PD targets of 26.8% for bacteriostasis, 30.7% for a 1-$\log_{10}$ CFU reduction, and 34.7% for a 2-$\log_{10}$ CFU reduction (13, 51). These targets were determined based on unbound serum concentrations. To evaluate which dose provided better coverage for susceptibility profiles of MRSA isolates encountered in clinical practice, PTAs were compared with ceftaroline MIC frequency distributions reported on the EUCAST MIC distribution website (https://mic.eucast.org/).

Data availability. The raw data analyzed during the current study are available from the authors upon reasonable request.

SUPPLEMENTAL MATERIAL

Supplemental material is available online only.

SUPPLEMENTAL FILE 1, PDF file, 5.7 MB.

ACKNOWLEDGMENTS

We thank the Coordenação de Aperfeiçoamento de Pessoal de Nível Superior-Brazil (CAPES) and the National Council for Scientific and Technological Development (CNPq) for research grants. T.D.C. and A.P.Z. are research fellows of the CNPq, Ministry of Science and Technology, Brazil. This work was funded by research grants from the CNPq/Brazil, CAPES finance code 001, and Pfizer (2018 Anti-Infectives ASPIRE, number WI242215).

A.P.Z., B.V.d.A., and T.D.C. have received research grants from Pfizer.

REFERENCES

1. Riccobene TA, Carrothers TJ, Knebel W, Raber S, Chan PLS. 2021. Pharmacokinetic and pharmacodynamic target attainment in adult and pediatric patients following administration of ceftaroline fosamil as a 5-minute infusion. Clin Pharmacol Drug Dev 10:420–427. https://doi.org/10.1002/cpdd.907.
2. Scott LJ. 2016. Ceftaroline fosamil: a review in complicated skin and soft tissue infections and community-acquired pneumonia. Drugs 76:1659–1674. https://doi.org/10.1007/s40265-016-0654-4.
3. Lakhundi S, Zhang K. 2018. Methicillin-resistant Staphylococcus aureus: molecular characterization, evolution, and epidemiology. Clin Microbiol Rev 31:e00020-18. https://doi.org/10.1128/CMR.00020-18.
4. Sakoulas G, Nonejuie P, Kullar R, Pogliano J, Rybak MJ, Nizet V. 2015. Examining the use of ceftaroline in the treatment of Streptococcus pneumoniae meningitis with reference to human cathelicidin LL-37. Antimicrob Agents Chemother 59:2428–2431. https://doi.org/10.1128/AAC.04965-14.
5. Pani A, Colombo F, Agnelli F, Frantellizzi V, Baratta F, Pastori D, Scaglione F. 2019. Off-label use of ceftaroline fosamil: a systematic review. Int J Antimicrob Agents 54:562–571. https://doi.org/10.1016/j.ijantimicag.2019.06.025.
6. Tong SYC, Davis JS, Eichenberger E, Holland TL, Fowler VG, Jr. 2015. Staphylococcus aureus infections: epidemiology, pathophysiology, clinical manifestations, and management. Clin Microbiol Rev 28:603–661. https://doi.org/10.1128/CMR.00134-14.
7. Cies JJ, Moore WS, Enache A, Chopra A. 2020. Ceftaroline cerebrospinal fluid penetration in the treatment of a ventriculopleural shunt infection: a case report. J Pediatr Pharmacol Ther 25:336–339. https://doi.org/10.5863/1551-6776-25.4.336.
8. Roujansky A, Martin M, Gomart C, Hulin A, Mounier R. 2020. Multidrug-resistant Staphylococcus epidermidis ventriculostomy-related infection successfully treated by intravenous ceftaroline after failure of daptomycin treatment. World Neurosurg 136:221–225. https://doi.org/10.1016/j.wneu.2020.01.013.
9. Chauzy A, Nadji A, Combes JC, Defrance N, Bouhemad B, Couet W, Chavanet P. 2019. Cerebrospinal fluid pharmacokinetics of ceftaroline in neurosurgical patients with an external ventricular drain. J Antimicrob Chemother 74:675–681. https://doi.org/10.1093/jac/dky489.
10. Matzneller P, Lackner E, Lagler H, Wulkersdorfer B, Österreicher Z, Zeitlinger M. 2016. Single- and repeated-dose pharmacokinetics of ceftaroline in plasma and soft tissues of healthy volunteers for two different dosing regimens of ceftaroline fosamil. Antimicrob Agents Chemother 60:3617–3625. https://doi.org/10.1128/AAC.00097-16.
11. Riccobene TA, Pushkin R, Jandourek A, Knebel W, Khariton T. 2016. Penetration of ceftaroline into the epithelial lining fluid of healthy adult subjects. Antimicrob Agents Chemother 60:5849–5857. https://doi.org/10.1128/AAC.02755-15.
12. van Wart SA, Ambrose PG, Rubino CM, Khariton T, Riccobene TA, Friedland HD, Critchley IA, Bhavnani SM. 2014. Pharmacokinetic-pharmacodynamic target attainment analyses to evaluate in vitro susceptibility test interpretive criteria for ceftaroline against Staphylococcus aureus and Streptococcus pneumoniae. Antimicrob Agents Chemother 58:885–891. https://doi.org/10.1128/AAC.01680-13.
13. Das S, Li J, Iaconis J, Zhou D, Stone GG, Yan JL, Melnick D. 2019. Ceftaroline fosamil doses and breakpoints for Staphylococcus aureus in complicated skin and soft tissue infections. J Antimicrob Chemother 74:425–431. https://doi.org/10.1093/jac/dky439.
14. Asín-Prieto E, Rodríguez-Gascón A, Isla A. 2015. Applications of the pharmacokinetic/pharmacodynamic (PK/PD) analysis of antimicrobial agents. J Infect Chemother 21:319–329. https://doi.org/10.1016/j.jiac.2015.02.001.
15. Nielsen EI, Friberg LE. 2013. Pharmacokinetic-pharmacodynamic modeling of antibacterial drugs. Pharmacol Rev 65:1053–1090. https://doi.org/10.1124/pr.111.005769.
16. Shah DK, Betts AM. 2012. Towards a platform PBPK model to characterize the plasma and tissue disposition of monoclonal antibodies in preclinical species and human. J Pharmacokinet Pharmacodyn 39:67–86. https://doi.org/10.1007/s10928-011-9232-2.
17. Johanson CE, Duncan JA, III, Klinge PM, Brinker T, Stopa EG, Silverberg GD. 2008. Multiplicity of cerebrospinal fluid functions: new challenges in health and disease. Cerebrospinal Fluid Res 5:10. https://doi.org/10.1186/1743-8454-5-10.
18. van Wart SA, Forrest A, Khariton T, Rubino CM, Bhavnani SM, Reynolds DK, Riccobene T, Ambrose PG. 2013. Population pharmacokinetics of ceftaroline in patients with acute bacterial skin and skin structure infections or community-acquired bacterial pneumonia. J Clin Pharmacol 53:1155–1167. https://doi.org/10.1002/jcph.153.
19. Riccobene TA, Khariton T, Knebel W, Das S, Li J, Jandourek A, Carrothers TJ, Bradley JS. 2017. Population PK modeling and target attainment simulations to support dosing of ceftaroline fosamil in pediatric patients with acute bacterial skin and skin structure infections and community-acquired bacterial pneumonia. J Clin Pharmacol 57:345–355. https://doi.org/10.1002/jcph.809.
20. Riccobene T, Jakate A, Rank D. 2014. A series of pharmacokinetic studies of ceftaroline fosamil in select populations: normal subjects, healthy elderly subjects, and subjects with renal impairment or end-stage renal disease requiring hemodialysis. J Clin Pharmacol 54:742–752. https://doi.org/10.1002/jcph.265.
21. Gonçalves-Pereira J, Póvoa P. 2011. Antibiotics in critically ill patients: a systematic review of the pharmacokinetics of β-lactams. Crit Care 15:R206. https://doi.org/10.1186/cc10441.
22. Roberts JA, Kirkpatrick CMJ, Roberts MS, Dalley AJ, Lipman J. 2010. First-dose and steady-state population pharmacokinetics and pharmacodynamics of piperacillin by continuous or intermittent dosing in critically ill

patients with sepsis. Int J Antimicrob Agents 35:156–163. https://doi.org/10.1016/j.ijantimicag.2009.10.008.
23. Jalusic KO, Hempel G, Arnemann PH, Spiekermann C, Kampmeier TG, Ertmer C, Gastine S, Hessler M. 2021. Population pharmacokinetics of vancomycin in patients with external ventricular drain-associated ventriculitis. Br J Clin Pharmacol 87:2502–2510. https://doi.org/10.1111/bcp.14657.
24. Xiao AJ, Miller BW, Huntington JA, Nicolau DP. 2016. Ceftolozane/tazobactam pharmacokinetic/pharmacodynamic-derived dose justification for phase 3 studies in patients with nosocomial pneumonia. J Clin Pharmacol 56:56–66. https://doi.org/10.1002/jcph.566.
25. Ding J, Thuy Thuong Thuong N, Pham TV, Heemskerk D, Pouplin T, Tran CTH, Nguyen MTH, Nguyen PH, Phan LP, Nguyen CVV, Thwaites G, Tarning J. 2020. Pharmacokinetics and pharmacodynamics of intensive antituberculosis treatment of tuberculous meningitis. Clin Pharmacol Ther 107:1023–1033. https://doi.org/10.1002/cpt.1783.
26. Lu C, Zhang Y, Chen M, Zhong P, Chen Y, Yu J, Wu X, Wu J, Zhang J. 2016. Population pharmacokinetics and dosing regimen optimization of meropenem in cerebrospinal fluid and plasma in patients with meningitis after neurosurgery. Antimicrob Agents Chemother 60:6619–6625. https://doi.org/10.1128/AAC.00997-16.
27. Chow E, Troy SB. 2014. The differential diagnosis of hypoglycorrhachia in adult patients. Am J Med Sci 348:186–190. https://doi.org/10.1097/MAJ.0000000000000217.
28. Nau R, Sörgel F, Eiffert H. 2010. Penetration of drugs through the blood-cerebrospinal fluid/blood-brain barrier for treatment of central nervous system infections. Clin Microbiol Rev 23:858–883. https://doi.org/10.1128/CMR.00007-10.
29. Kumta N, Roberts JA, Lipman J, Wong WT, Joynt GM, Cotta MO. 2021. A systematic review of studies reporting antibiotic pharmacokinetic data in the cerebrospinal fluid of critically ill patients with uninflamed meninges. Antimicrob Agents Chemother 65:e01998-20. https://doi.org/10.1128/AAC.01998-20.
30. Liu C, Bayer A, Cosgrove SE, Daum RS, Fridkin SK, Gorwitz RJ, Kaplan SL, Karchmer AW, Levine DP, Murray BE, Rybak MJ, Talan DA, Chambers HF. 2011. Clinical practice guidelines by the Infectious Diseases Society of America for the treatment of methicillin-resistant Staphylococcus aureus infections in adults and children. Clin Infect Dis 52:e18–e55. https://doi.org/10.1093/cid/ciq146.
31. Blassmann U, Hope W, Roehr AC, Frey OR, Vetter-Kerkhoff C, Thon N, Briegel J, Huge V. 2019. CSF penetration of vancomycin in critical care patients with proven or suspected ventriculitis: a prospective observational study. J Antimicrob Chemother 74:991–996. https://doi.org/10.1093/jac/dky543.
32. Ricard J-D, Wolff M, Lacherade J-C, Mourvillier B, Hidri N, Barnaud G, Chevrel G, Bouadma L, Dreyfuss D. 2007. Levels of vancomycin in cerebrospinal fluid of adult patients receiving adjunctive corticosteroids to treat pneumococcal meningitis: a prospective multicenter observational study. Clin Infect Dis 44:250–255. https://doi.org/10.1086/510390.
33. Taheri M, Dadashzadeh S, Shokouhi S, Ebrahimzadeh K, Sadeghi M, Sahraei Z. 2018. Administration of vancomycin at high doses in patients with post neurosurgical meningitis: a comprehensive comparison between continuous infusion and intermittent infusion. Iran J Pharm Res 17:195–205.
34. Marchand S, Chauzy A, Dahyot-Fizelier C, Couet W. 2016. Microdialysis as a way to measure antibiotics concentration in tissues. Pharmacol Res 111:201–207. https://doi.org/10.1016/j.phrs.2016.06.001.
35. Deitchman AN, Derendorf H. 2014. Measuring drug distribution in the critically ill patient. Adv Drug Deliv Rev 77:22–26. https://doi.org/10.1016/j.addr.2014.08.014.
36. Gonzalez D, Schmidt S, Derendorf H. 2013. Importance of relating efficacy measures to unbound drug concentrations for anti-infective agents. Clin Microbiol Rev 26:274–288. https://doi.org/10.1128/CMR.00092-12.
37. Viallon A, Botelho-Nevers E, Zeni F. 2016. Clinical decision rules for acute bacterial meningitis: current insights. Open Access Emerg Med 8:7–16. https://doi.org/10.2147/OAEM.S69975.
38. Kiang TKL, Häfeli UO, Ensom MHH. 2014. A comprehensive review on the pharmacokinetics of antibiotics in interstitial fluid spaces in humans: implications on dosing and clinical pharmacokinetic monitoring. Clin Pharmacokinet 53:695–730. https://doi.org/10.1007/s40262-014-0152-3.
39. Sauermann R, Delle-Karth G, Marsik C, Steiner I, Zeitlinger M, Mayer-Helm BX, Georgopoulos A, Müller M, Joukhadar C. 2005. Pharmacokinetics and pharmacodynamics of cefpirome in subcutaneous adipose tissue of septic patients. Antimicrob Agents Chemother 49:650–655. https://doi.org/10.1128/AAC.49.2.650-655.2005.
40. Barbour A, Scaglione F, Derendorf H. 2010. Class-dependent relevance of tissue distribution in the interpretation of anti-infective pharmacokinetic/pharmacodynamic indices. Int J Antimicrob Agents 35:431–438. https://doi.org/10.1016/j.ijantimicag.2010.01.023.
41. Rohatgi A. 2021. WebPlotDigitizer. Version 4.5.
42. Beal SL, Sheiner LB, Boeckmann AJ, Bauer RJ. 2022. NONMEM 7.4 users guides.
43. Keizer RJ, Karlsson MO, Hooker A. 2013. Modeling and simulation workbench for NONMEM: tutorial on Pirana, PsN, and Xpose. CPT Pharmacometrics Syst Pharmacol 2:e50. https://doi.org/10.1038/psp.2013.24.
44. Lindbom L, Pihlgren P, Jonsson EN. 2005. PsN-Toolkit—a collection of computer intensive statistical methods for non-linear mixed effect modeling using NONMEM. Comput Methods Programs Biomed 79:241–257. https://doi.org/10.1016/j.cmpb.2005.04.005.
45. Jonsson EN, Karlsson MO. 1999. Xpose—an S-PLUS based population pharmacokinetic/pharmacodynamic model building aid for NONMEM. Comput Methods Programs Biomed 58:51–64. https://doi.org/10.1016/S0169-2607(98)00067-4.
46. Tunblad K, Hammarlund-Udenaes M, Jonsson EN. 2004. An integrated model for the analysis of pharmacokinetic data from microdialysis experiments. Pharm Res 21:1698–1707. https://doi.org/10.1023/b:pham.0000041468.00587.c6.
47. Mould DR, Upton RN. 2013. Basic concepts in population modeling, simulation, and model-based drug development—part 2: introduction to pharmacokinetic modeling methods. CPT Pharmacometrics Syst Pharmacol 2:e38. https://doi.org/10.1038/psp.2013.14.
48. Nguyen THT, Mouksassi M-S, Holford N, Al-Huniti N, Freedman I, Hooker AC, John J, Karlsson MO, Mould DR, Pérez Ruixo JJ, Plan EL, Savic R, van Hasselt JGC, Weber B, Zhou C, Comets E, Mentré F, Model Evaluation Group of the International Society of Pharmacometrics (ISoP) Best Practice Committee. 2017. Model evaluation of continuous data pharmacometric models: metrics and graphics. CPT Pharmacometrics Syst Pharmacol 6:87–109. https://doi.org/10.1002/psp4.12161.
49. Byon W, Smith MK, Chan P, Tortorici MA, Riley S, Dai H, Dong J, Ruiz-Garcia A, Sweeney K, Cronenberger C. 2013. Establishing best practices and guidance in population modeling: an experience with an internal population pharmacokinetic analysis guidance. CPT Pharmacometrics Syst Pharmacol 2:e51. https://doi.org/10.1038/psp.2013.26.
50. Macey R, Oster G, Zahnley T. 2003. Berkeley Madonna user's guide. University of California, Berkeley, CA.
51. Cristinacce A, Wright JG, Stone GG, Hammond J, McFadyen L, Raber S. 2019. A retrospective analysis of probability of target attainment in community-acquired pneumonia: ceftaroline fosamil versus comparators. Infect Dis Ther 8:185–198. https://doi.org/10.1007/s40121-019-0243-4.